RESEARCH ARTICLE

Predicting resilient modulus of recycled concrete and clay masonry blends for pavement applications using soft computing techniques

Mosbeh R. KALOOP[a,b,c], Alaa R. GABR[c], Sherif M. EL-BADAWY[c], Ali ARISHA[c], Sayed SHWALLY[c], Jong Wan HU[a,b]*

[a] *Department of Civil and Environmental Engineering, Incheon National University, Incheon 22012, South Korea*

[b] *Incheon Disaster Prevention Research Center, Incheon National University, Incheon 22012, South Korea*

[c] *Department of Public Works and Civil Engineering, Mansoura University, Mansoura 35516, Egypt*

* *Corresponding author. E-mail: jongp24@incheon.ac.kr*

ABSTRACT   To date, very few researchers employed the Least Square Support Vector Machine (LSSVM) in predicting the resilient modulus (M_r) of Unbound Granular Materials (UGMs). This paper focused on the development of a LSSVM model to predict the M_r of recycled materials for pavement applications and comparison with other different models such as Regression, and Artificial Neural Network (ANN). Blends of Recycled Concrete Aggregate (RCA) with Recycled Clay Masonry (RCM) with proportions of 100/0, 90/10, 80/20, 70/30, 55/45, 40/60, 20/80, and 0/100 by the total aggregate mass were evaluated for use as UGMs. RCA/RCM materials were collected from dumps on the sides of roads around Mansoura city, Egypt. The investigated blends were evaluated experimentally by routine and advanced tests and the M_r values were determined by Repeated Load Triaxial Test (RLTT). Regression, ANN, and LSSVM models were utilized and compared in predicting the M_r of the investigated blends optimizing the best design model. Results showed that the M_r values of the investigated RCA/RCM blends were generally increased with the decrease in RCM proportion. Statistical analyses were utilized for evaluating the performance of the developed models and the inputs sensitivity parameters. Eventually, the results approved that the LSSVM model can be used as a novel tool to estimate the M_r of the investigated RCA/RCM blends.

KEYWORDS   Least Square Support Vector Machine, Artificial Neural Network, resilient modulus, Recycled Concrete Aggregate, Recycled Clay Masonry

1   Introduction

Recycling of Construction and Demolition (C&D) waste materials such as Recycled Concrete Aggregate (RCA) and Recycled Clay Masonry (RCM) is a unique sustainable application in the construction industry of buildings and infrastructures. The C&D waste harms the environment and the civilized face of the cities. They involve large costs for hauling to landfills in addition to the large landfill areas required for dumping. In addition, virgin materials are getting scarce and require quarrying, processing, and hauling for long distances sometimes, which consume

more energy and pollute the environment. Therefore, recycling such waste materials can solve these problems. In Egypt, the amounts of C&D waste materials increase dramatically every year (currently about 4 million tons/year), which cause environmental problems and affect people's life [1]. Therefore, Arisha [1] and Arisha et al. [2] evaluated the suitability of using RCA/RCM blends as Unbound Granular Materials (UGMs) in pavement construction in Egypt. Worldwide, numerous studies investigated the feasibility of using C&D waste materials in either flexible or rigid pavements' layers, i.e., Refs. [3,4]. For example, Gabr and Cameron [3] found that RCA materials were suitable for use as base material in pavement applications. On the other hand, Malešev et al. [4] assessed

the use of RCA as a construction material in the structural concrete production, which exhibited satisfied results in terms of mechanical properties compared to virgin aggregates. However, they recommended that precaution should be considered for structures exposed to water due to the alkali-silica reaction. In summary, most of the literature published studies evaluated the use of RCA and RCM materials as UGMs investigating the index engineering properties and resilient modulus and recommended the use of it as either base or subbase material. More details about the conducted studies on C&D waste materials can be found in Refs. [1,5].

The resilient modulus (M_r) is a key design parameter for the characterization of pavement materials and pavement design [3,6]. M_r is estimated in the laboratory by the Repeated Load Triaxial Test (RLTT), which can be used to assess how the pavement system responds under cyclic traffic loadings [6]. M_r can be correlated with stress state, i.e., deviator stress and bulk stress, or can be correlated with the engineering properties of the material such as California Bearing Ratio (CBR) [7]. The development of M_r prediction models is important to study the impact of dynamic traffic loading on material's behavior and to save time consumed during testing as well as testing costs.

Andrei et al. [7], Ji et al. [8], George [9], Arisha et al. [2], Lekarp et al. [10], and Mousa et al. [11] summarized most of the available published M_r regression models for the UGMs and subgrade soils. The most well-known model for predicting M_r as a function of stress state only is the universal model presented in Eq. (1) [12].

$$M_r = K_1 P_a \left(\frac{\theta}{P_a} \right)^{K_2} \left(\frac{\tau}{P_a} + 1 \right)^{K_3}, \qquad (1)$$

where M_r is the resilient modulus; K_1, K_2, and K_3 are the material regression coefficients; θ is the bulk stress $= \sigma_1 + \sigma_2 + \sigma_3$; σ_1 is the major principal stress; σ_2 is the minor principal stress; σ_3 is the isotropic confining pressure; τ is the octahedral shear stress $= \frac{1}{3}\sqrt{(\sigma_1-\sigma_2)^2 + (\sigma_1-\sigma_3)^2 + (\sigma_2-\sigma_3)^2}$; and finally, P_a is the atmospheric pressure ($P_a = 101.3$ kPa).

Arisha et al. [2] modified Eq. (1) by incorporating the RCM content to predict the resilient modulus of RCA/RCM blends as follows:

$$M_r = K_1 P_a \left(\frac{\theta}{P_a} \right)^{K_2} \left(\frac{\tau}{P_a} + RCM \cdot A \right)^{K_3}, \qquad (2)$$

where K_1, K_2, K_3, and A are the regression coefficients; RCM is the content of masonry brick, %.

On the other hand, Kim et al. [13], Sadrossadat et al. [14], Reza and Rahrovan [15] recommended the Artificial Neural Network (ANN) technique to predict the M_r of base materials and subgrade soils. Zaman et al. [16] utilized the ANN model to predict the M_r for the subgrade soil and they

found that the prediction accuracy in terms of the coefficient of determination (R^2) for the ANN model was 0.58. Elbagalati et al. [17] used the ANN to predict the M_r for the flexible pavement behavior, and they found that the accuracy of the model design (R^2) was 0.72. Kim et al. [13] found that the prediction accuracy of the ANN M_r model for subgrade soils in terms of R^2 is 0.86. Reza and Rahrovan [15] compared the ANN model with two other techniques, Support Vector Regression (SVR) and least square methods for the prediction of M_r of stabilized base materials. They found that the ANN prediction accuracy of M_r is better than the other two methods ($R^2 = 0.98$). Sadrossadat et al. [14] developed a M_r prediction model for subgrade soils using the Adaptive Neuro-Fuzzy Inference System (ANFIS), which is an integrated method of both fuzzy and ANN, and found that the ANFIS model is a good tool for M_r prediction ($R^2 = 0.97$). Based on the literature review, it can be concluded that the accuracy of ANN is changed based on the input parameters and ANN characteristics. More details for the ANN model design and properties can be found in Refs. [13,17,18].

Recently, the Least Square Support Vector Machine (LSSVM) method is getting more attention from research in establishing prediction models in different engineering areas [19–21]. The LSSVM is a developed approach rather than the SVR in the regression models, which require a higher computational burden to make the optimization of data [22]. LSSVM is superior on other techniques in estimating the behavior of smart structures [23]. Samui et al. [24] compared ANN and LSSVM models for the prediction of swelling pressure and found that the prediction performance of LSSVM method is better than the ANN method. Kaloop and Hu [23] found that the prediction performances of the LSSVM model is better than the ANFIS model for identifying the behavior of base isolation movement. More information about the regression and evolutionary soft computing techniques used for the waste production, material behavior and infrastructure modeling are detailed with more case studies by Fardad et al. [25], Hamdia et al. [26,27], Badawy et al. [28], and Gopalakrishnan et al. [29].

Most of the published M_r prediction models used the regression with least square solution or ANNs, but very few attempts, to author's knowledge, have been made to use the LSSVM in predicting the M_r of UGMs. In this study, two different modeling techniques, ANN and LSSVM were used and evaluated for the prediction of M_r, which were compared with the regression model presented in Eq. (2) for RCA/RCM materials. Equation (2) [2] was developed by modifying the universal model, Eq. (1) [12], considering the most important factors that affects the prediction of resilient modulus such as stress state ($\frac{\theta}{P_a}$ and $\frac{\tau}{P_a}$) and the RCM percentage. The independent and dependent variables of Eq. (2) were
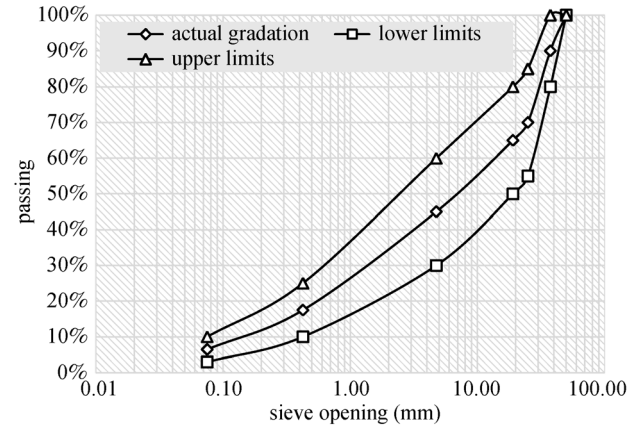
kept the same in modeling the other two techniques, ANN and LSSVM for comparison and simplification of the model.

2 Materials and methods

RCA and RCM were extracted from the dumps on the road sides around Mansoura city, Egypt and then crushed (Fig. 1) in the Highway and Airport Engineering laboratory, Mansoura University, to small particles with maximum size of 50 mm. After that, the crushed materials were sieved to achieve one target gradation for all blends as required by the Egyptian Code of Practice (ECP) for UGMs [30] as shown in Fig. 2. The percentages of the RCA/RCM blends were 100/0, 90/10, 80/20, 70/30, 55/45, 40/60, 20/80, and 0/100 of the total aggregate mass.

The conducted experimental program was divided into two main parts, routine testing and advanced testing. The routine tests include Atterberg limits, AASHTO classification, Maximum Dry Density (MDD) and Optimum Moisture Content (OMC), Los Angeles Abrasion (LAA), CBR, specific gravity, water absorption, pH, and hydraulic conductivity. The advanced tests included the determination of resilient modulus, M_r and shear strength parameters, cohesion (c) and angle of internal friction (ϕ). In addition,

Scanning Electron Microscopy (SEM), Energy Dispersive Spectroscopy (EDS), and X-ray Diffraction (XRD) were conducted to determine the microstructure and chemical composition of the RCA/RCM samples before and after blending.

Fig. 2 Particle size distribution for investigated blends. Reprinted from Procedia Engineering, 143, Ali Arisha, Alaa Gabr, Sherif El-Badawy, Sayed Shwally, Using Blends of Construction & Demolition Waste Materials and Recycled Clay Masonry Brick in Pavement, 8, Copyright (2016), with permission from Elsevier.
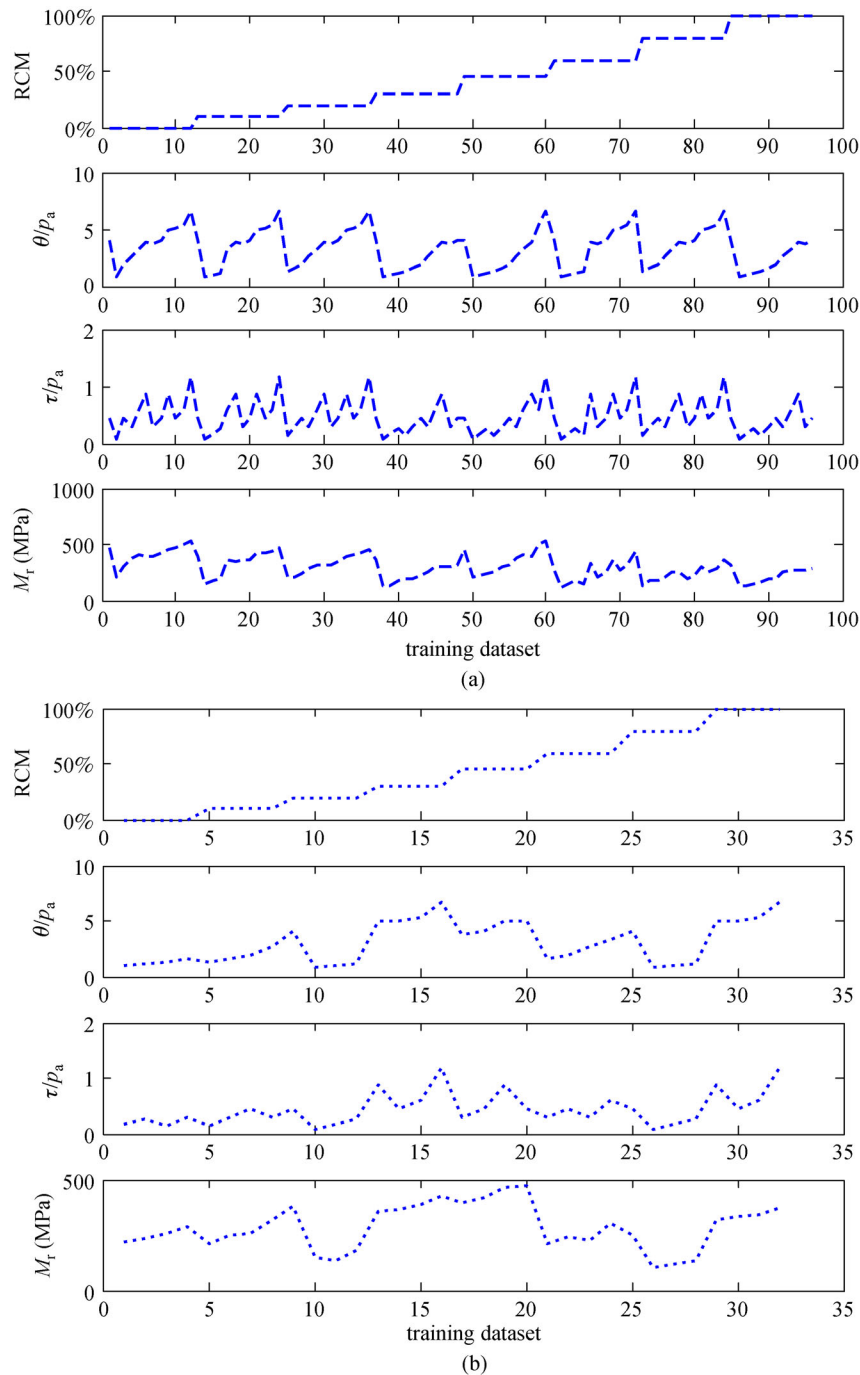

Fig. 1 Crushing of RCA/RCM materials [30]. (a) RCA before crushing; (b) RCM before crushing; (c) RCA after crushing; (d) RCM after crushing.

2.1 Modeling M_r

The measured M_r values from the RLTT test (128 points) were divided into training (96 points) and testing (32 points) data sets, as presented in Fig. 3. All inputs used in Eq. (2) for M_r prediction were also used as the main input parameters for the investigated techniques. Table 1 illustrates the statistical analysis results (maximum, minimum, mean, and standard deviation (SD)) of the

parameters used in M_r prediction for each of the training and testing data sets. Figure 3 showed that the variation of data for each parameter between training and testing data was not much different and the ranges of data for each parameter were almost similar for both sets. Table 1 evidenced the observation from the figure that the training and testing sets were almost populated with comparable values of SD.

Fig. 3 Training and testing datasets. (a) Training dataset; (b) testing dataset.

Table 1   Statistical analysis for the training and testing data sets

data set	item	RCM (%)	$\dfrac{\theta}{P_a}$	$\dfrac{\tau}{P_a}$	M_r (MPa)
training dataset	max	100.000	6.619	1.170	527.80
	min	0.000	0.807	0.088	114.95
	mean	43.130	3.283	0.473	296.41
	SD	32.860	1.681	0.290	106.95
testing dataset	max	100.000	6.619	1.170	475.00
	min	0.000	0.807	0.088	101.95
	mean	43.130	3.072	0.431	285.83
	SD	33.209	1.887	0.287	102.849

2.2   Prediction models and performance methods

In this study, three methods were utilized and compared, first is the regression model, which was developed by Arisha et al. [2]. Second is the ANN model, which is expected to yield better predictions according to Kim et al. [13], and finally the LSSVM, which is being used for first time to predict the M_r of the UGMs. The following is a brief summary of each method utilized.

First, Arisha et al. [2] developed the regression model presented in Eq. (2) based on the RLTT data for all RCA/RCM blends (128 points). The regression coefficients, K_1, K_2, K_3, and A were optimized for all RCA/RCM blends by applying Eq. (2) to all RLTT data using nonlinear numerical optimization through the solver function in Microsoft Excel [2].

Second, the ANN model was used to predict the M_r values of the RCA/RCM blends. From the mathematical overview of ANN theory, the ANN mainly contains three layers, which are input, hidden and output layers [13,31]. ANN with one hidden layer was adopted in this study. Each layer contains one or more neurons; three inputs and one output neuron structures are utilized in this case. However, the main factors that affect ANN accuracy are the weight parameters, which depend on the number of hidden neurons, and the activation function. The sigmoid function $f(\cdot)$ was adopted based on Kim et al. [13] results for the hidden layer and the linear function $F(\cdot)$ was used for the output layer, as presented in Eq. (3).
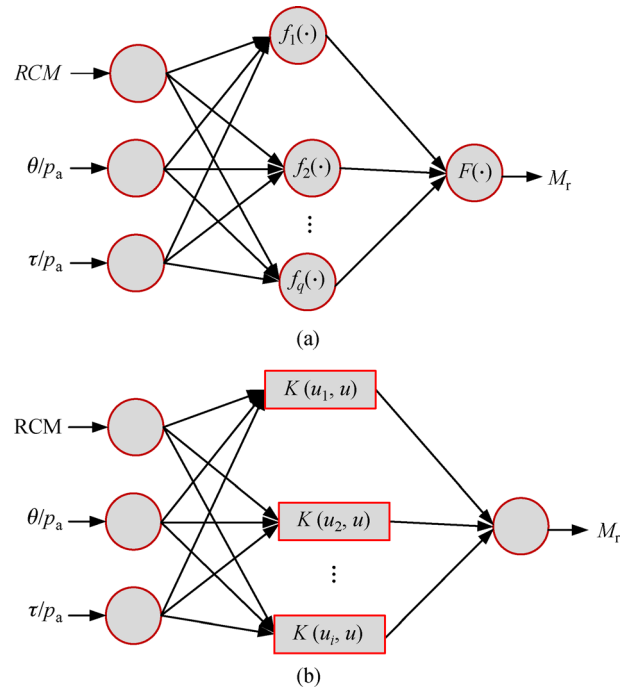
Figure 4(a) shows the chosen ANN model structure in this study. M_r can be predicted by using the ANN (3-N-1), where N is the number of hidden layers. The ANN M_r model presented in Fig. 4(a) can be described as follows:

$$M_{ri} = F_i\left(\sum_{j=0}^{q} W_{ij} f_j\left(\sum_{l=1}^{m} w_{jl} z_l + w_{j0}\right) + W_{i0}\right), \quad (3)$$

where w and W are the weights for the connections between input-hidden and hidden-output layers, respectively, w_{j0}, W_{i0} are the bias parameters for the hidden and output neurons, respectively, q and m are the number of output and hidden neurons, respectively. The training data

are a set of inputs ($u(i)$) and corresponding desired outputs $M_r(i)$; the training set can be specified by $z^n = \{[u(i), M_r(i)]|i = 1,...,n\}$ [32].

The feed-forward neural network was applied to adjust the connection weight according to learning rules, which minimizes the error function between the observed and predicted values [13,32]. One hidden layer was chosen in this study to compare the results of ANN with LSSVM in the same conditions, while the LSSVM contained also three layers, as presented in Fig. 4.

(a)

(b)

Fig. 4   (a) ANN and (b) LSSVM models' diagram.

The LSSVM is the third method that was investigated in this study as a new tool for the prediction of M_r of the RCA/RCM materials. The LSSVM theory is detailed by Suykens and Vandewalle [22] and Samui et al. [33].

Figure 4(b) illustrates the LSSVM structure.

To predict M_r of RCA/RCM materials, the three parameters, RCM, $(\frac{\theta}{P_a})$, and $(\frac{\tau}{P_a})$ were considered as inputs. These inputs were denoted as $u_i \in R^n$ and the output was described as $M_{ri} \in r$; where R^n is the n-dimensional vector data and r is the one-dimensional output data. The LSSVM can take the following form between input and output variables:

$$M_{ri} = w^T \varphi(u_i) + b + e_i, \qquad (4)$$

where $\varphi(u)$ is a nonlinear function in-between input and output data. w is an adjustable weight vector, b is a scalar threshold, and e is the model error.

To extract the map function, two steps were followed. The first step was the application of the minimization principal by penalizing a regression error as presented in Eq. (5). Second, Eqs. (4) and (5) should be optimized using the Lagrange multipliers method by the application of Eq. (6).

$$J(w,e) = 0.5w^T w + 0.5\gamma \sum_{i=1}^{n} e_i^2, \qquad (5)$$

$$L(w,b,e,\alpha) = J(w,e) - \sum_{i=1}^{n} \alpha_i \{ w^T \varphi(u_i) + b + e_i - M_{ri} \},$$

where γ is the regularization parameter; and α is the Lagrange multiplier.

Therefore, the final form of M_r model for the RCA/RCM materials can be described as follows:

$$M_{ri} = \sum_{i=1}^{n} \alpha_i K(u_i, u) + b, \qquad (7)$$

where K is the activation function. In this study, the radial basis function (RBF) was used, which can be given by:

$$K(u_i, u_c) = \exp\left\{ -\frac{[u_i - u_c]^T [u_i - u_c]}{2\sigma^2} \right\}, i,c = 1,2,...,n, \qquad (8)$$

where σ is the width of RBF.

The performance of the investigated models was evaluated by four statistical measures, which are the coefficient of determination (R^2), Root Mean Square Error ($RMSE$), and adjusted coefficient of efficiency (E). R^2 is used to measure the fitness between the measured and predicted values, while $RMSE$ is used to describe the average magnitude of the model errors by giving more weight on large error, E gives the absolute difference between the measured and predicted values relative to the absolute mean of observed data, and mean absolute error (MAE) describes the average and magnitude of the model errors [34]. The four measures are described in the following equations:

$$R^2 = \left[\frac{\sum_{i=1}^{n} (M_{rio} - M_{rmo})(M_{rip} - M_{rmp})}{\sqrt{\sum_{i=1}^{n} (M_{rio} - M_{rmo})^2 \sum_{i=1}^{n} (M_{rip} - M_{rmp})}} \right]^2, \qquad (9)$$

$$RMSE = \sqrt{\frac{\sum_{i=1}^{n} (M_{rio} - M_{rip})^2}{2}}, \qquad (10)$$

$$E = 1 - \frac{\sum_{i=1}^{n} |M_{rio} - M_{rip}|}{\sum_{i=1}^{n} |M_{rio} - M_{rmo}|}, \qquad (11)$$

$$MAE = \frac{1}{n} \sum_{i=1}^{n} |M_{rio} - M_{rip}|, \qquad (12)$$

where M_{rio} and M_{rip} are the measured and predicted M_r values at the ith step; M_{rmo} and M_{rmp} are the mean of M_r for the measured and predicted values.

Furthermore, the linear fitting was utilized to estimate the best fitting between observation and prediction M_r values. The linear fitting can be presented as: $y = ax + b$; while y and x are the predicted and observed M_r, respectively, a and b are the slope and constant of linear fitting parameters. The best fitting is obtained when the a is 1 and b is 0, otherwise the fitting quality is minimal.

A summary of the conducted methodology for predicting M_r using the three different models is presented in Fig. 5. This methodology for the three models was processed through four stages: collection of the materials, determination the material properties, and the measurements of the M_r values; development of the three models; performance study and comparison between the prediction models; selection of the best model that can be used to estimate the M_r.

3 Results and discussions

3.1 Results of laboratory testing

Table 2 summarizes the results of the engineering properties of the RCA/RCM blends as well as the shear strength parameters. The table also provides the RLTT results represented by the K_1, K_2, and K_3 regression coefficients of Eq. (1) along with the standard deviation for the investigated materials. These regression coefficients were determined by the nonlinear optimization of the RLTT testing results using Eq. (1) with the help of the Solver function in Microsoft Excel. It can be seen from the table
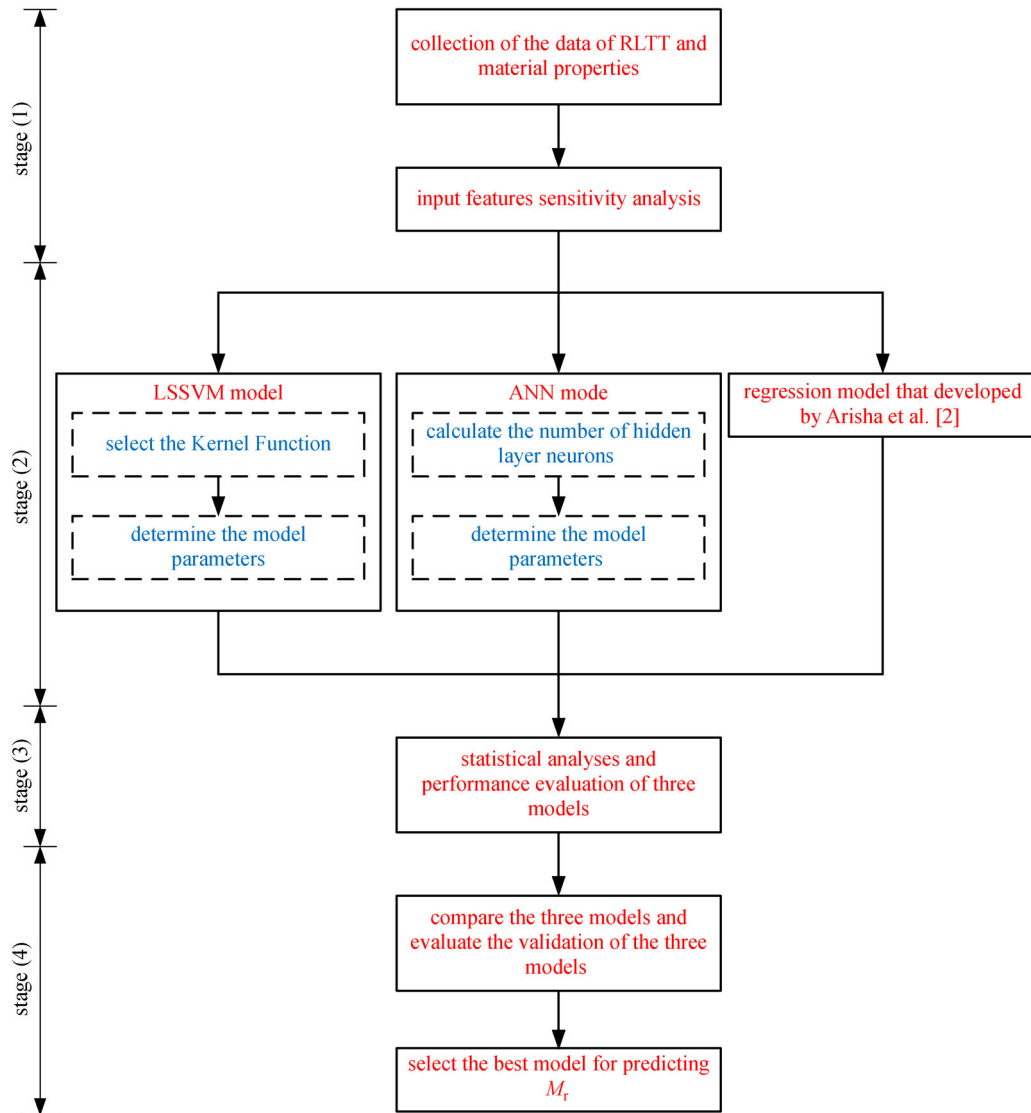
Fig. 5 Flowchart of stages processing for modeling M_r.

that the eight RCA/RCM met the Egyptian specifications [22] for UGMs, nevertheless the LAA surpassed for RCM blends (10% to 100%) the ECP limits. The shear strength of the eight investigated RCA/RCM blends was not affected by the RCM content. The resilient modulus of the eight RCA/RCM blends was generally increased by the decrease in RCM content. Resilient modulus and CBR was improved due to the self-cementing nature of RCA than RCM samples as confirmed further by the XRD results.

Table 3 and Fig. 6 [35] show an example of the chemical composition of the investigated materials conducted by XRD. The table reveals that the dominant mineral phases in the original RCA powder were Quartz, Dolomite, Calcite, and Albite, while in the RCA powder after mixing as shown in the figure; new chemical reactions were occurred forming different morphology with a new mineral phase, Microcline. On the other hand, the composition of

the mineral phases for the original and mixed RCM powders were different as given in the table with the main compounds as Quartz, Albite, Microcline, and Hematite. The new mineral phases were formed inside the blended samples due to the hydration process yielding different morphology than the original sample. In-depth discussion of all conducted testing and the general engineering properties including the resilient modulus data and the assessment of the RCA/RCM blends are detailed in Refs. [1,2,28].

3.2 Modeling results

The sensitivity analysis between output and each input variable was statistically investigated using the Cosine Amplitude Method (CAM) for the development of prediction models Ref. [14]. For more detail about the

Table 2　Summary of the engineering properties of RCA/RCM blends [35]

property		test result							
material (RCA/RCM)		100/0	90/10	80/20	70/30	55/45	40/60	20/80	0/100
OMC		12.7%	14.4%	13.5%	14.3%	11.5%	12.4%	10.1%	10.8%
MDD (t/m^3)		1.86	1.84	1.82	1.82	1.84	1.84	1.78	1.75
liquid limit		25%	–	–	–	–	–	–	26%
plasticity index		NP*	–	–	–	–	–	–	NP*
AASHTO classification		A-1-a							A-1-a
CBR		152.9%	128.7%	114.5%	114.5%	119.4%	114.5%	69.5%	76.6%
LAA		47.2%	–	–	–	–	–	–	83.8%
pH		9.1	–	–	–	–	–	–	8.8
K (m/s)		1.8E–08	–	–	–	7.7E–09	–	–	1.5E–07
water absorption		0.80%	–	–	–	–	–	–	7.20%
specific gravity (Gs)		2.30	–	–	–	–	–	–	2.03
apparent cohesion, c, (kPa)		12.4	25.8	56.8	89.2	80.3	24.0	50.9	43.1
friction Angle, ϕ		58.4°	55.6°	52.7°	48.8°	53.2°	59.7°	50.4°	52.7°
M_r (Eq. (1))	K_1	2.29 ± 0.270	1.85 ± 0.437	1.62 ± 0.325	1.50 ± 0.033	2.31 ± 0.251	1.34 ± 0.099	1.15 ± 0.090	1.45 ± 0.086
	K_2	0.49 ± 0.037	0.53 ± 0.163	0.59 ± 0.121	0.57 ± 0.018	0.48 ± 0.027	0.19 ± 0.011	0.37 ± 0.032	0.57 ± 0.007
	K_3	−0.134 ± 0.004	−0.09 ± 0.031	−0.099 ± 0.019	−0.056 ± 0.001	−0.124 ± 0.028	1.073 ± 0.003	0.548 ± 0.005	−0.194 ± 0.001
	R^2	0.974	0.981	0.976	0.975	0.975	0.960	0.972	0.981

*Note: NP: Non plastic.

Table 3　XRD results for RCA and RCM before and after mixing

mineral phase	original RCA	RCA after mixing	original RCM	RCM after mixing
Quartz	39%	37.6%	64.8%	55.4%
Dolomite	27.8%	31.2%	–	–
Calcite	22.3%	14.4%	–	–
Albite	10.9%	–	19.4%	17.6%
Microcline	–	16.8%	9.7%	23.4%
Hematite	–	–	6.1%	3.6%

CAM calculation and evaluation can be found in Ref. [14] and for the global sensitivity analyses about the identification models can be referred to Hamdia et al. [27]. The strength ratio (r) was used to measure the strength correlation between input and output variables; as the r value close to one means that the effectiveness of the input variable is high with predicted M_r values. Figure 7 shows the conducted sensitivity analysis by the strength ratio on the three incorporated inputs in this study with the measured values of M_r for all collected data.
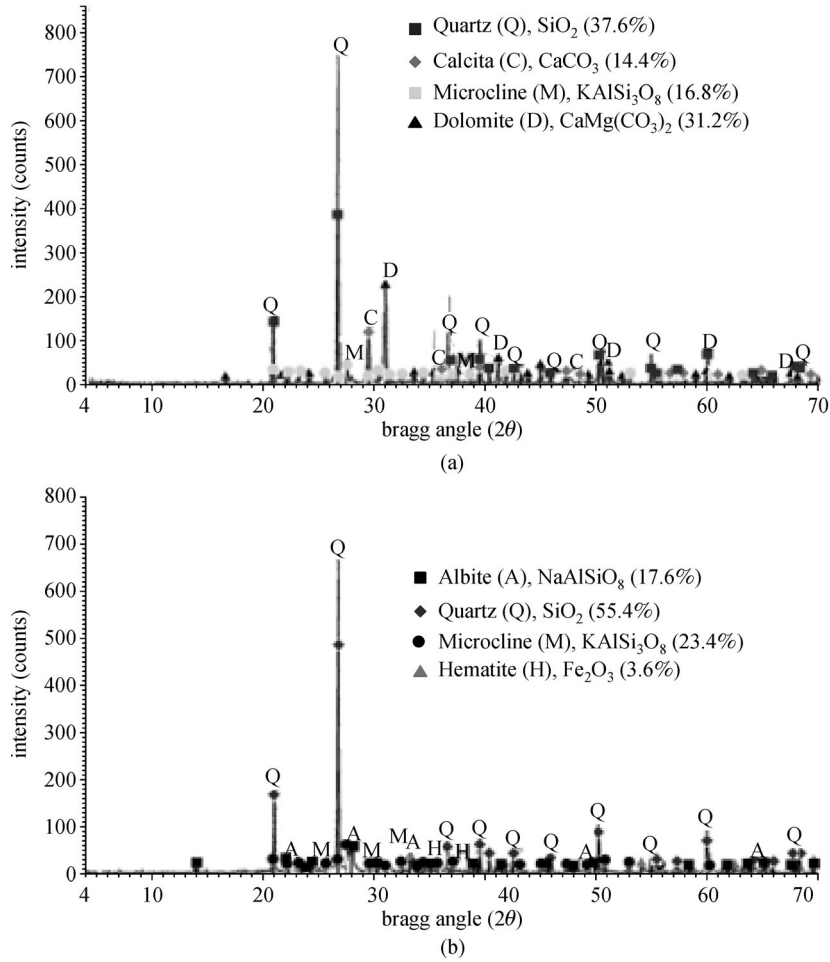
From Fig. 7, the sensitivity of the three input variables were high correlated and affect the prediction of M_r. The sensitivity of bulk stress, θ and octahedral shear stress, τ was higher than the RCM content. Nevertheless, Arisha et al. [35] showed that the RCM content in the regression model (Eq. (2)) is an important input variable to correlate the resilient modulus for all RCA/RCM blends, otherwise

the prediction accuracy and bias increase. Therefore, the three input variables were kept the same as in Eq. (2) and were adopted for the other two prediction models, ANN and LSSVM to explore the best model that would be used to predict M_r for all RCA/RCM blends.
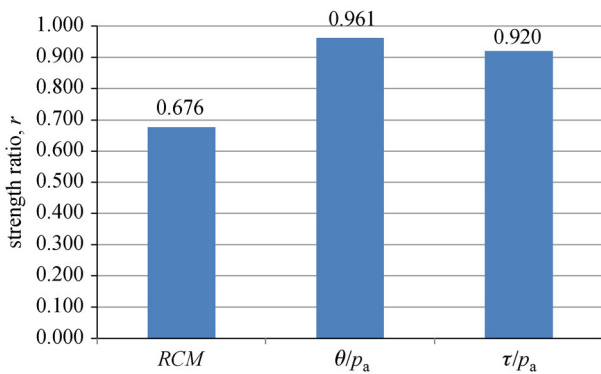
3.2.1　Evaluation of the investigated models

Equation (2) was first optimized in the arithmetic space by the nonlinear numerical optimization function (Solver) in Microsoft Excel, as presented in Arisha et al. [2,35]. The values of the regression coefficients, K_1, K_2, K_3, and A, for all RCA/RCM blends were found to be 1.85, 0.54, −0.13, and 0.08, respectively.

To investigate the ANN prediction model, the number of hidden neurons and the weight matrix should be first explored and evaluated as shown earlier in Eq. (4). The

(a)

(b)

Fig. 6   XRD analysis for (a) RCA and (b) RCM sample after mixing Reprinted from Ref. [35] with permission from Journal of Materials in Civil Engineering.

Fig. 7   Sensitivity analysis of input parameters.

Table 4   Statistics measures for the number of ANN hidden neurons

No. of neurons	4	8	10	15	20
R^2	0.819	0.839	0.901	0.910	0.915
$RMSE$ (MPa)	45.279	42.646	33.429	31.913	30.951

neurons affected the performance of the ANN prediction model. It should be noted that the complexity of the ANN model increases when the number of neurons increases. Therefore, based on the $RMSE$ and R^2 measures presented in Table 4, the change in the performance of the ANN model was low for the hidden neurons between 10 and 20. In this study, the 10 hidden neurons were selected to design the ANN prediction model for RCA/RCM blends and to be compared with other investigated models. Hence, the structure of the ANN prediction model was 3 inputs, 10 hidden neurons, and one output (3-10-1). To validate the model design, the mean square error (MSE) of the training model was used up to 0.01 MPa. Figure 8(a) presents the validation of the training design model using 1000 iteration to reach the target MSE. In addition, Fig. 8(b) illustrates

trial and error theory was used to estimate the number of the hidden neurons. In addition, the gradient descend method was utilized to estimate the weight connection values between the ANN layers [13]. Table 4 shows the five attempts to estimate the hidden neuron numbers.

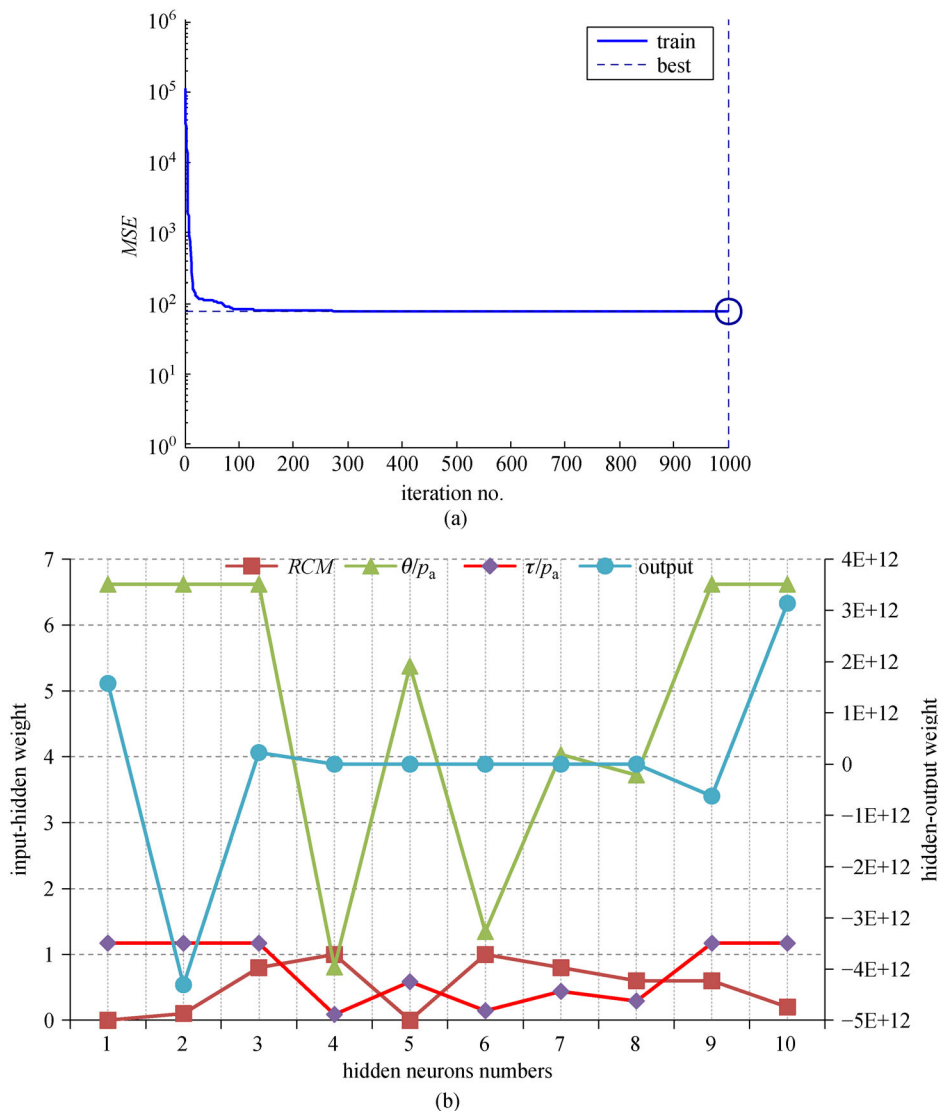It can be seen from Table 4 that the number of hidden

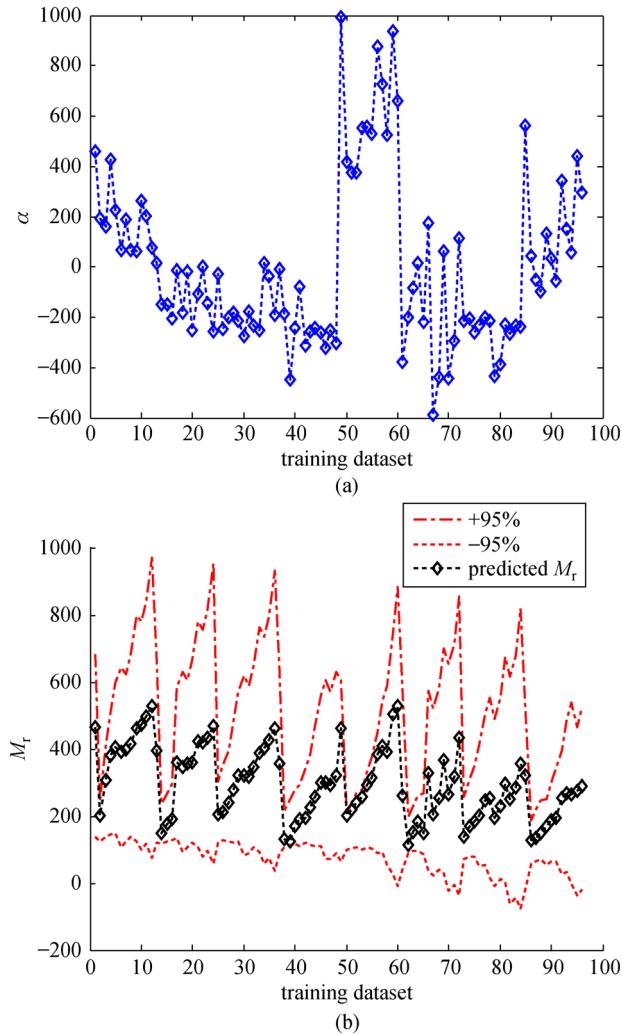Fig. 8   (a) MSE model validation and (b) Input-hidden and hidden-output weights values.

Table 5   Statistics measures of the three prediction models for the training and testing data sets

model	training set				testing set			
	R^2	RMSE (MPa)	MAE (MPa)	E	R^2	RMSE (MPa)	MAE (MPa)	E
Reg.	0.817	45.715	31.915	0.644	0.868	38.770	25.988	0.699
ANN	0.901	33.429	24.888	0.722	0.887	34.805	27.297	0.685
LSSVM	0.848	41.473	32.744	0.635	0.982	13.768	10.555	0.878

the weight matrix estimation of input-hidden and hidden-output neurons based on the 10 selected hidden neurons. Moreover, the bias was found to be 0.166 for the hidden neurons and -3559.638 for the output neuron.

The LSSVM model was designed using RBF kernel function, Eq. (8), which was designed based on four parameters that were γ, σ, α, and b as presented earlier in Eqs. (5) to (8). The trial and error algorithm was utilized to estimate the values of these parameters. In addition, the 95% error-band was used to estimate the best model that can be used to predict the M_r values. Figure 9 presents the best estimated α values for determining the best design (Fig. 9(a)) and the 95% error-band of the training data set of the LSSVM model (Fig. 9(b)). The values of the LSSVM coefficients, γ, σ^2, and b for RCA/RCM blends were found to be 54.315, 1.811, and -3.585, respectively.

Fig. 9 LSSVM model design (a) α value, (b) training 95% error band.

It should be mentioned that the polynomial kernel function was assessed, and it was found that the *RMSE* of RBF and polynomial functions were 42.473 and 42.475 MPa, respectively, which means that the performance of the two functions were close in predicting M_r.
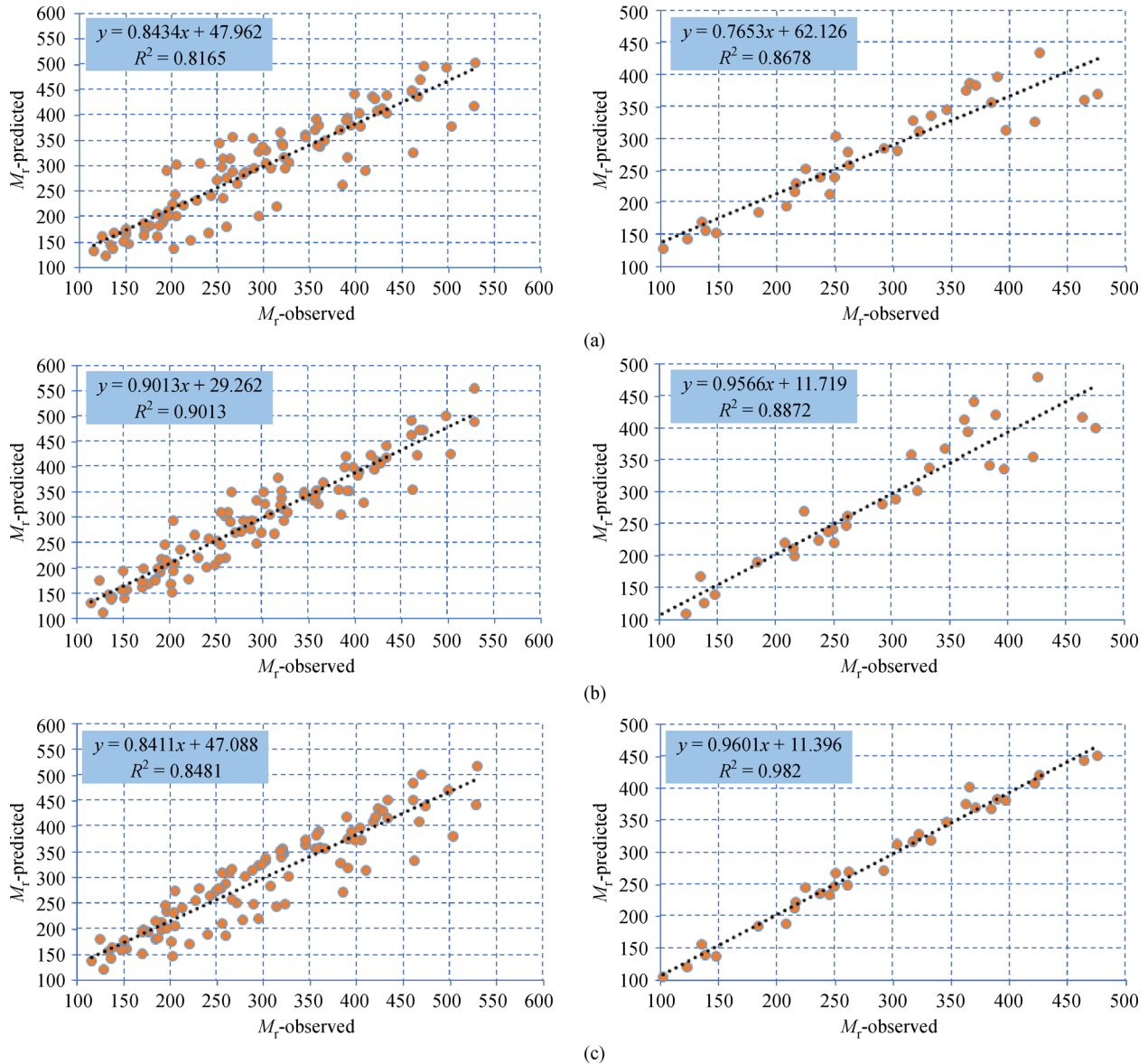
Figure 10 depicts the measured versus predicted M_r values as well as the prediction accuracy of the three investigated models for training and testing data sets. Table 5 gives a summary of the statistical measures of the three investigated models for both training and testing data. In addition, the linear fitting between observed and predicted values of M_r is presented in Fig. 10. It can be seen from both Fig. 10 and Table 5 that the prediction accuracy in terms of R^2, *RMSE*, and *AME* for the training set of Eq. (2) was 0.817, 45.72, and 31.915 MPa, respectively. While, the prediction accuracy increased by 26.87% and 9.28% for the ANN and LSSVM models for the same data set with lower *RMSE* of 33.43 and 41.47, respectively. Moreover, the adjusted coefficient of

efficiency, E and *MAE* increased by 12.11% and 22.02%, respectively, for the ANN model and decreased by 1.4% and 2.59%, respectively, for the LSSVM model compared with Eq. (2). However, the predicted M_r values from LSSVM model using the training data set were within the error-band interval as shown in Fig. 9(b). Furthermore, the linear fitting in training stage showed that the slope and constant parameters were 0.9013 and 29.262, respectively, for the ANN model and these parameters were smallest for the three models. In essence, the ANN prediction model was the best model for predicting M_r values during the training stage for RCA/RCM blends. On the other hand, the LSSVM model was enhanced significantly with the highest E of 0.88 becoming the best prediction model compared with the other two models during the testing stage with R^2 of 0.982 as evidenced from Fig. 10 and Table 5. As well, the prediction accuracy in term of RMSE of ANN and LSSVM increased by 10.23% and 64.49%, respectively, compared to the regression model for the testing stage. The *MAE* of LSSVM was improved by 59.39% in comparison with the regression model. In addition, the slope linear fitting parameter for the ANN and LSSVM was 0.957 and 0.960, respectively, and the constant was 11.719 and 11.396 for the ANN and LSSVM, respectively. It means that the performance of the LSSVM prediction model was better with lower number of data. While for the ANN model, data should be large for better accuracy, which agreed with the results published by Gopalakrishnan et al. [29] but not for the M_r prediction for UGMs.

In conclusion, the main advantage of the regression model (Eq. (2)) is that it improved the prediction accuracy compared to the universal model (Eq. (1)) in addition to its simplicity, while it was not completely capable to predict M_r values justifiably [2,35]. The ANN model improved significantly the M_r prediction values in both training and testing stages compared to the regression model. Nevertheless, it seems that large database is needed to improve the ANN predictions. LSSVM model is seen better for the training and testing datasets compared to the regression model, and it was the best model with lowest number of M_r measurements. However, further investigation should be conducted in the future on larger materials with datasets outside the investigated ranges to judge on the capability of the LSSVM for larger database.

4   Summary and conclusions

This study addressed advanced methodologies for predicting resilient modulus of RCA/RCM materials based on RLTT results. These advanced methodologies were ANN and LSSVM approaches, which were compared with a regression model (Eq. (2)). The concepts behind these approaches and the fundamental advantages of each were presented. The sensitivity and estimated properties of the

Fig. 10 Predicted versus measured M_r for RCA/RCM blends, Regression, ANN, and LSSVM fit for training (left) and testing (right) data sets: (a) Regression; (b) ANN; (c) LSSVM.

designed input and output variables were studied and evaluated. In this context, the following conclusions can be drawn:

The resilient modulus of the eight RCA/RCM blends was improved with the reduction in RCM content owing to the self-cementing nature of RCA than RCM as evidenced by XRD. The sensitivity analysis showed that the three investigated parameters (bulk stress, octahedral shear stress, and RCM content) have a significant effect on the prediction performance for the three investigated M_r predictive models.

Equation (2) is a modified version to the universal model (Eq. (1)) that predicts the resilient modulus as function of stress state and RCM content. The model was found to

have good prediction accuracy for all blends with R^2 of 0.82. The evaluations of the developed regression, ANN, and LSSVM models exhibited that the three investigated models can be used to predict the M_r value for the RCA/RCM blends. However, the ANN and LSSVM models were better than the regression model developed by Arisha et al. [2,35]. Moreover, the ANN model had better M_r predictions with large number of M_r measurements (training stage), while the LSSVM model performed better in the testing stage with lower number of data. Finally, it can be concluded that the LSSVM is a powerful technique that can be employed for the M_r prediction for only RCA/RCM materials, which requires further validation for larger data sets.

References

1. Arisha A. Evaluation of recycled clay masonry blends in pavement construction. Thesis for the Master's Degree. Mansoura: Mansoura University, 2017

2. Arisha A, Gabr A, El-Badawy S, Shwally S. Using blends of construction & demolition waste materials and recycled clay masonry brick in pavement. Procedia Engineering, 2016, 143: 1317–1324

3. Gabr A, Cameron D. Properties of recycled concrete aggregate for unbound pavement construction. Journal of Materials in Civil Engineering, 2012, 24(6): 754–764

4. Malešev M, Radonjanin V, Marinković S. Recycled concrete as aggregate for structural concrete production. Sustainability, 2010, 2(5): 1204–1225

5. Cardoso R, Silva R V, Brito J, Dhir R. Use of recycled aggregates from construction and demolition waste in geotechnical applications: A literature review. Waste Management (New York), 2016, 49: 131–145

6. Mousa E, Azam A, El-Shabrawy M, El-Badawy S. Laboratory characterization of reclaimed asphalt pavement for road construction in Egypt. Canadian Journal of Civil Engineering, 2017, 44(6): 417–425

7. Andrei D, Witczak M, Houston W. Resilient modulus predictive model for unbound pavement materials. In: International Foundation Congress and Equipment Expo 2009, 2009, 401–408

8. Ji R, Siddiki N, Nantung T, Kim D. Evaluation of resilient modulus of subgrade and base materials in Indiana and its implementation in MEPDG. The Scientific World Journal, 2014, 2014: 1–14

9. George K. Prediction of Resilient Modulus from Soils Index Proprieties. 2004

10. Lekarp F, Isacsson U, Dawson A. State of the art. I: Resilient response of unbound aggregates. Journal of Transportation Engineering, 2000, 126(1): 66–75

11. Mousa R, Gabr A, Arab M, Azam A, El-Badawy S. Resilient modulus for unbound granular materials and subgrade soils in Egypt. In: Proceedings of the International Conference on Advances in Sustainable Construction Materials & Civil Engineering Systems, 2017

12. AASHTO. Mechanistic-Empirical Pavement Design Guide: A Manual of Practice. Interim Edition, American Association of Highways and Transportation Officials. 2008

13. Kim S, Yang J, Jeong J. Prediction of subgrade resilient modulus using artificial neural network. KSCE Journal of Civil Engineering, 2014, 18(5): 1372–1379

14. Sadrossadat E, Heidaripanah A, Osouli S. Prediction of the resilient modulus of flexible pavement subgrade soils using adaptive neuro-fuzzy inference systems. Construction & Building Materials, 2016, 123: 235–247

15. Reza A, Rahrovan M. Application of artificial neural network to predict the resilient modulus of stabilized base subjected to wet dry cycles. Computations and Materials in Civil Engineering, 2016, 1 (1): 37–47

16. Zaman M, Solanki P, Ebrahimi A, White L. Neural network modeling of resilient modulus using routine subgrade soil properties. International Journal of Geomechanics, 2010, 10(1): 1–12

17. Elbagalati O, Elseifi M A, Gaspard K, Zhang Z. Development of an artificial neural network model to predict subgrade resilient modulus from continuous deflection testing. Canadian Journal of Civil Engineering, 2017, 44(9): 700–706

18. Solanki P, Zaman M, Ebrahimi A. Regression and artificial neural network modeling of resilient modulus of subgrade soils for pavement design applications. Intelligent and Soft Computing in Infrastructure Systems Engineering, 2009, 259: 269–304

19. Zuo R, Carranza E. Support vector machine: A tool for mapping mineral prospectivity. Computers & Geosciences, 2011, 37(12): 1967–1975

20. van Gestel T, Suykens J A K, Baesens B, Viaene S, Vanthienen J, Dedene G, de Moor B, Vandewalle J. Benchmarking least squares support vector machine classifiers. Machine Learning, 2004, 54(1): 5–32

21. Samui P, Kothari D. Utilization of a least square support vector machine (LSSVM) for slope stability analysis. Scientia Iranica, 2011, 18(1): 53–58

22. Suykens J, Vandewalle J. Least squares support vector machine classifiers. Neural Processing Letters, 1999, 9(3): 293–300

23. Kaloop M, Hu J. Seismic response prediction of buildings with base isolation using advanced soft computing approaches. Advances in Materials Science and Engineering, 2017, 2017: 7942782

24. Samui P, Das S, Sitharam T. Application of soft computing techniques to expansive soil characterization. In: Intelligent and Soft Computing in Infrastructure Systems Engineering, 2009, 305–306

25. Fardad K, Najafi B, Ardabili S F, Mosavi A, Shamshirband S, Rabczuk T. Biodegradation of medicinal plants waste in an anaerobic digestion reactor for biogas production. Computer, Material and Continua, 2018, 55(3): 318–392

26. Hamdia K M, Ghasemi H, Zhuang X, Alajlan N, Rabczuk T. Sensitivity and uncertainty analysis for flexoelectric nanostructures. Computer Methods in Applied Mechanics and Engineering, 2018, 337: 95–109

27. Hamdia K M, Silani M, Zhuang X, He P, Rabczuk T. Stochastic analysis of the fracture toughness of polymeric nanoparticle composites using polynomial chaos expansions. International Journal of Fracture, 2017, 206(2): 215–227

28. Badawy M F, Msekh M A, Hamdia K M, Steiner M K, Lahmer T, Rabczuk T. Hybrid nonlinear surrogate models for fracture behavior of polymeric nanocomposites. Probabilistic Engineering Mechanics, 2017, 50: 64–75

29. Gopalakrishnan K, Ceylan H, Attoh-Okine N. Intelligent and Soft Computing in Infrastructure Systems Engineering. 2009

30. ECP. Egyptian Code of Practice for Urban and Rural Roads, Edition 1: Road Materials and Their Tests (Part Four). The Ministry of Housing, Utilities and Urban Communities, Egypt, 2008

31. Brey T. A multi-parameter artificial neural network model to estimate macrobenthic invertebrate productivity and production. Limnology and Oceanography, Methods, 2012, 10(8): 581–589

32. Norgaard M, Ravn O, Poulsen N K. NNSYSID-toolbox for system identification with neural networks. Mathematical and Computer Modelling of Dynamical Systems, 2002, 8(1): 1–20

33. Samui P, Kim D, Aiyer B. Pullout capacity of small ground anchor: A least square support vector machine approach. Journal of Zhejiang University. Science A, 2015, 16(4): 295–301

34. Karimi S, Kisi O, Shiri J, Makarynskyy O, Shiri1 J, Makarynskyy O. A wavelet and neuro-fuzzy conjunction model to forecast air temperature variations at coastal sites. The International Journal of Ocean and Climate Systems, 2015, 6(4): 159–1721

35. Arisha A, Gabr A, El-badawy S, Shwally S. Performance evaluation of construction and demolition waste materials for pavement construction in Egypt. Journal of Materials in Civil Engineering, 2018, 30(2): 04017270